

# Clustering of heavy particles in the inertial range of turbulence

J. Bec,<sup>1</sup> M. Cencini,<sup>2,3</sup> and R. Hillerbrand<sup>1,4</sup>

<sup>1</sup>*CNRS UMR 6202, Observatoire de la Côte d'Azur, BP4229, 06304 Nice Cedex 4, France.*

<sup>2</sup>*CNR, Istituto dei Sistemi Complessi, Via dei Taurini 19, 00185 Roma, Italy.*

<sup>3</sup>*INFN-SMC c/o Dip. di Fisica Università Roma 1, P.zzle A. Moro 2, 00185 Roma, Italy.*

<sup>4</sup>*Institut für theoretische Physik, Westfälische Wilhelms-Univ., Münster, Germany.*

(Dated: August 7, 2018)

A statistical description of heavy particles suspended in incompressible rough self-similar flows is developed. It is shown that, differently from smooth flows, particles do not form fractal clusters. They rather distribute inhomogeneously with a statistics that only depends on a local Stokes number, given by the ratio between the particles' response time and the turnover time associated to the observation scale. Particle clustering is reduced when increasing the fluid roughness. Heuristic arguments supported by numerics are used to explain this effect in terms of the algebraic tails of the probability density function of the velocity difference between two particles. These tails are a signature of events during which particle couples approach each other very closely.

PACS numbers: 47.27.-i, 47.51.+a, 47.55.-t

In turbulent flow, finite-size particles heavier than the carrier fluid, as e. g. water droplets in air, possess inertia and have a finite response time to the fluid motion. Thus their dynamics markedly differs from that of simple tracers and, in particular, such inertial particles distribute in a strongly inhomogeneous manner even if the underlying flow is incompressible. Modelling these fluctuations in the particle concentration is important in engineering [1], cloud physics [2], and planetology [3].

The turbulent motion of the carrier fluid spans many active spatial and temporal scales [4]. Below the Kolmogorov length-scale, viscous dissipation dominates; the velocity field is differentiable and is characterized by a single time scale. There the motion of inertial particles is governed by the fluid strain and their dissipative dynamics leads their trajectories to converge to a dynamically evolving attractor. For any given response time of the particles, their mass distribution is singular and generically scale-invariant with multifractal properties at small scales [5, 6, 7]. Above the Kolmogorov scale, the fluid velocity field is not smooth anymore but, according to the Kolmogorov 1941 theory, almost self-similar with Hölder exponent  $h = 1/3$  [4]. This so-called inertial range is characterized by a broad-spectrum of time scales. However, the finite response time of the suspended particles introduces a new scale, breaking self-similarity in the particle distribution. This is consistent with the observation that particles typically concentrate on different scales with the largest deviation from uniformity arising when their response time is of the order of the eddy turnover time [8, 9]. As already noticed in [7], these deviations are not scale-invariant and have a different origin from those observed in the viscous range of turbulence. With few exceptions [10, 11, 12], clustering in the inertial range received considerably less attention than small-scale clustering.

In this Letter we focus on second-order statistics of the

particle distribution at scales within the inertial range. These statistics can be completely described in terms of the relative motion of particle pairs. Within the inertial range, two concurrent mechanisms responsible for particle clustering can be identified: a dissipative dynamics due to their viscous drag with the fluid and ejection from persistent vortical regions by centrifugal forces [13]. By modelling the carrier flow as a rough, self-similar random velocity field which is  $\delta$ -correlated in time, we eliminate the latter effect: the absence of any persistent structure in the considered carrier flow ensures that centrifugal forces play no role. This model pertains to *very* heavy particles whose response time is much larger than the typical correlation time of the ambient fluid [14, 15]. We show heuristically and numerically that the scale-invariance of the velocity field does not extend to the particle distribution, and that roughness of the carrier velocity weakens clustering. This effect is explained by the dependence of the relative velocity distribution on the fluid velocity Hölder exponent.

The relative motion of two particles is described by their separation  $\mathbf{R}$  that obeys the equation [13, 14]

$$\ddot{\mathbf{R}} = -\frac{1}{\tau} \left[ \dot{\mathbf{R}} - \delta \mathbf{u}(\mathbf{R}, t) \right], \quad (1)$$

where the dots denote time derivatives,  $\tau$  is the Stokes time, and  $\delta \mathbf{u}(\mathbf{r}, t) = \mathbf{u}(\mathbf{x} + \mathbf{r}, t) - \mathbf{u}(\mathbf{x}, t)$  is the fluid velocity difference. The velocity  $\mathbf{u}$  is assumed to be a stationary, homogeneous and isotropic Gaussian field with correlation

$$\langle u_i(\mathbf{x}, t) u_j(\mathbf{x}', t') \rangle = 2D_0 \delta_{ij} - B_{ij}(\mathbf{x} - \mathbf{x}') \delta(t - t'), \quad (2)$$

where  $D_0$  is the velocity variance. For rough self-similar flows, the function  $B$  takes the form

$$B_{ij}(\mathbf{r}) = D_1 r^{2h} [(d-1+2h)\delta_{ij} - 2hr_i r_j / r^2], \quad (3)$$

where  $r = |\mathbf{r}|$ ,  $d$  is the space dimension,  $h \in [0, 1]$  the Hölder exponent of the carrier velocity field, and  $D_1$  a

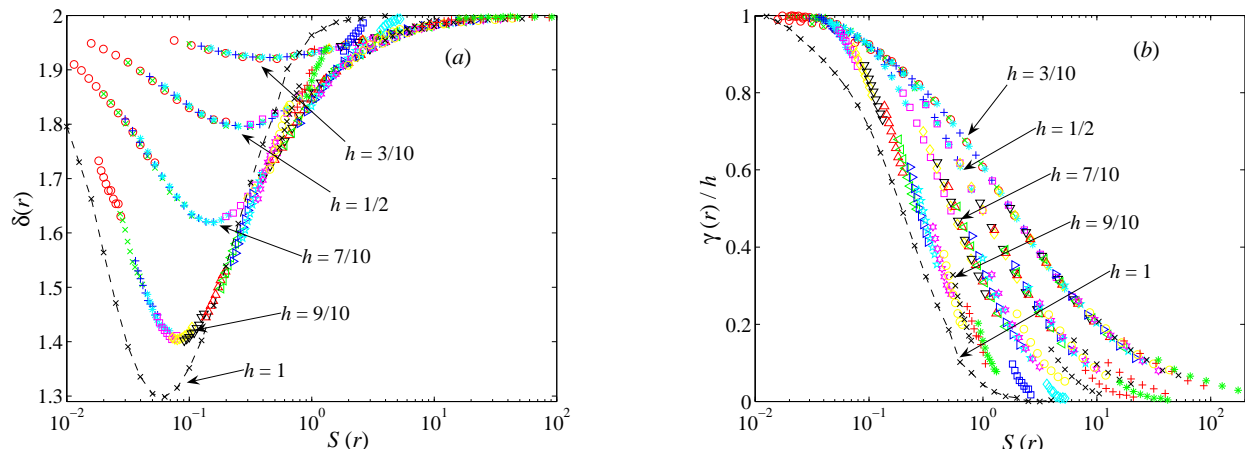


FIG. 1: (a) Local correlation dimension  $\delta(r)$  versus the scale-dependent Stokes number  $\mathcal{S}(r) = D_1\tau/r^{2(1-h)}$  for various values of the Hölder exponent  $h$  in two dimensions  $d = 2$ . (b) Ratio between the local exponent  $\gamma(r)$  of the particle velocity and  $h$  versus  $\mathcal{S}(r)$ . Different symbols (colors online) refer to different values of the particle response time  $\tau$ .

constant measuring the intensity of turbulence. This kind of velocity field was introduced by Kraichnan [16] to model passive scalar transport.

By defining  $s = t/\tau$  and rescaling  $\mathbf{R}$  by the observation scale  $\ell$ , it is easily seen that the above dynamics, and thus all the statistical properties of particle pairs at scale  $\ell$  only depend on the *local Stokes number*  $\mathcal{S}(\ell) = D_1\tau/\ell^{2(1-h)}$ . This dimensionless quantity, first introduced in [9], is the ratio between the particle response time  $\tau$  and the turnover time at scale  $\ell$ . It measures the scale-dependent effects of inertia. At large scales ( $\ell \rightarrow \infty$ ) inertia becomes negligible ( $\mathcal{S}(\ell) \rightarrow 0$ ) and particles recover the incompressible dynamics of tracers. Conversely, since  $\mathcal{S}(\ell) \rightarrow \infty$  for  $\ell \rightarrow 0$ , inertia effects become dominant at small scales and the dynamics approaches that of free particles. For both very large and very small values of the Stokes number, the particles distribute uniformly in space. Strong inhomogeneities appear for  $\mathcal{S}(\ell) \approx 1$ .

Note that in unbounded carrier flows, the separation between two particles asymptotically grow indefinitely with time and thus the dynamics (1) never reaches a statistical steady state. However, real turbulent flows are bounded, allowing for statistical equilibrium to be reached. Boundary conditions are thus implemented in the considered model by imposing, for instance, reflection of the inter-particle distance at  $|\mathbf{R}| = L$ . Clearly, since self-similarity is broken by the presence of boundaries, the aforementioned scaling arguments apply only at scales  $\ell \ll L$ .

For smooth carrier flows ( $h = 1$ ), there is a unique time scale so that the dynamics only depends on the global Stokes number  $\mathcal{S} = D_1\tau$ . Inhomogeneities in the particle distribution can be quantified by  $d - \mathcal{D}_2$ , where  $\mathcal{D}_2$  is the *correlation dimension*

$$\mathcal{D}_2 = \lim_{r \rightarrow 0} \delta(r), \quad \delta(r) = d(\ln P_2(r)) / d(\ln r), \quad (4)$$

$P_2(r)$  denoting the probability that  $|\mathbf{R}| < r$ . In  $\delta$ -correlated smooth flows, just as in real suspensions, the correlation dimension  $\mathcal{D}_2$  non-trivially depends on the Stokes number [14].

For non-smooth but Hölder-continuous flows,  $\mathcal{D}_2 = d$  for *all* particle response times. Information on the inhomogeneities of the particle distribution is entailed in the local correlation dimension  $\delta(r)$  defined in (4). From above arguments,  $\delta(r)$  is expected to depend only on  $h$  and on the local Stokes number  $\mathcal{S}(r)$  when  $r \ll L$ . This is confirmed numerically for  $d = 2$  as shown in Fig. 1a, where the local dimension  $\delta(r)$  is represented as a function of  $\mathcal{S}(r)$ . The collapse of the data for various response times  $\tau$  demonstrates the dependence on the local Stokes number. Comparing various values of the exponent  $h$ , we observe that when the fluid becomes rougher, the intensity of clustering weakens. In particular, the minimum of  $\delta(r)$  gets closer to  $d = 2$  as  $h$  decreases. Notice that for  $h = 1$ , the Stokes number  $\mathcal{S}$  does not depend on  $r$  and data refer to the actual value of the correlation dimension, which is well defined for smooth flows (see [14] for details).

We now turn to the typical velocity difference  $\dot{\mathbf{R}}$  between two particles and its dependency on the separation  $\mathbf{R}$ . For smooth flows, when  $|\mathbf{R}| \rightarrow 0$  an algebraic behavior of the form  $|\dot{\mathbf{R}}| \sim |\mathbf{R}|^\gamma$  is observed, defining a Hölder exponent  $\gamma$  for the particle velocities. This exponent decreases from  $\gamma = h = 1$  for  $\mathcal{S} = 0$ , corresponding to a differentiable particle velocity field, to  $\gamma = 0$  for  $\mathcal{S} \rightarrow \infty$ , that means particle moving with uncorrelated velocities [14]. In non-smooth flows the exponent  $\gamma$  is asymptotically equal to the fluid Hölder exponent  $h$  at large scales ( $\mathcal{S}(r) \rightarrow 0$ ), while it approaches 0 at very small scales ( $\mathcal{S}(r) \rightarrow \infty$ ). Therefore, similarly to  $\delta(r)$ , all relevant information is entailed in the scale dependence of the local exponent  $\gamma(r)$ . As for the local correlation dimension, this exponent only depends on the fluid Hölder expo-

ment and on the local Stokes number; this is confirmed in Fig. 1b, showing the ratio  $\gamma(r)/h$  versus  $\mathcal{S}(r)$  for various values of  $h$ . It is worth noticing that the transition from  $\gamma(r) = h$  to  $\gamma(r) = 0$  shifts towards larger values of the local Stokes number and broadens as  $h$  decreases. The fact that  $\gamma(r) = h$  for  $r \rightarrow \infty$  implies that the particles should asymptotically experience Richardson diffusion [4] just as simple tracers.

To get a deeper understanding of the mechanisms of clustering, we transform the equations of motion (1)-(2) into a system of stochastic differential equations with additive noise. Adapting to rough flows the strategy first proposed in [17] for smooth carrier velocities fields and used in [18], we make the following change of variables:

$$\begin{aligned} X &= (\tau/L^2) (|\mathbf{R}|/L)^{-(1+h)} \mathbf{R} \cdot \dot{\mathbf{R}}, \\ Y &= (\tau/L^2) (|\mathbf{R}|/L)^{-(1+h)} |\mathbf{R} \wedge \dot{\mathbf{R}}|, \\ Z &= (|\mathbf{R}|/L)^{1-h}. \end{aligned} \quad (5)$$

The variables  $X$  and  $Y$  refer to the longitudinal and the transverse dimensionless velocity differences, respectively. When  $d = 2$ , the dynamics (1) in the four-dimensional phase-space  $(\mathbf{R}, \dot{\mathbf{R}})$  reduces to

$$\dot{X} = -X - Z^{-1} (hX^2 - Y^2) + \eta_1(s), \quad (6)$$

$$\dot{Y} = -Y - (1+h) Z^{-1} XY + \eta_2(s), \quad (7)$$

$$\dot{Z} = (1-h)X. \quad (8)$$

Now the dots denote derivatives with respect to  $s = t/\tau$ ;  $\eta_1$  and  $\eta_2$  are independent white noises with variances  $2\mathcal{S}(L)$  and  $2(1+2h)\mathcal{S}(L)$ , respectively;  $\mathcal{S}(L) = D_1 \tau/L^{2(1-h)}$  is the Stokes number associated with the system size. Periodic boundary conditions in physical space amount to considering reflective boundary conditions at  $Z = 1$ ;  $Y$  is ensured to remain positive by reflective boundary conditions at  $Y = 0$ . Rescaling  $|\mathbf{R}|$  with  $\lambda$ , and thus  $Z$  with  $\lambda^{1-h}$  leads to transform  $X$  and  $Y$  to  $\lambda^{1-h}X$  and  $\lambda^{1-h}Y$  in order to confine the scaling factor in the noise. This again amounts to considering the same dynamics with a scale-dependent Stokes number  $\mathcal{S}(\lambda L)$ . The system (6)-(8) can be efficiently implemented numerically and was used to produce the data described in this Letter.

Figure 2 sketches the dynamics in the  $(X, Y, Z)$  space. The line  $X = Y = 0$  (its physical meaning is that the particles have relaxed to the same velocity staying at an arbitrary distance) acts as a stable fixed line for the drift terms in (6)-(8). A typical trajectory spends a long time diffusing around this line, until the noise realization becomes strong enough to escape from its neighborhood. When this happens with  $X > 0$ , the quadratic terms in the drift drive the trajectory back to the stable line. On the contrary, if  $X < 0$  and  $hX^2 + XZ - Y^2 < 0$ , the drift accelerates the trajectory towards larger negative values of  $X$ . Then  $Z$  decreases until the quadratic terms in (6)-(7) become dominant. The trajectory then loops back in the

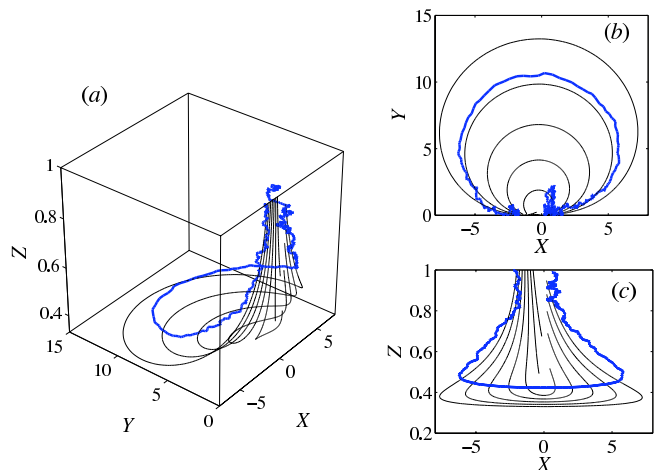


FIG. 2: Phase-space picture of the system (6)-(8) for  $h = 7/10$ . The thin smooth lines represent effects of the drift. A random trajectory of the system with  $\mathcal{S}(L) = 1$  is shown as a bold line; it performs a large loop from  $X < 0$  to  $X > 0$ . (a) The full  $(X, Y, Z)$  space, (b) and (c) projections in the  $Z = 0$  and  $Y = 0$  planes, respectively.

$(X, Y)$ -plane, approaching the stable line from its right. These loops are the events during which  $Z$  (and hence the inter-particle distance  $R$ ) becomes substantially small.

As we now show, these loops are responsible for power-law tails in the probability density function (PDF) of the dimensionless velocity differences  $X$  and  $Y$ . This behavior can be understood by extending to the rough case the arguments developed in [14] for smooth flows. For this we consider the cumulative probability  $P^<(x) = \Pr(X < x)$  with  $x \ll -1$ , which can be estimated as the product of (i) the probability to start a sufficiently large loop that reaches values more negative than  $x$  and (ii) the fraction of time spent by the trajectory at  $X < x$ . To estimate these two contributions, we assume that within a distance of order unity from the line  $X = Y = 0$  the quadratic terms in the drift are negligible, so that  $X$  and  $Y$  behave as two independent Ornstein-Uhlenbeck processes. At larger distances we retain only the quadratic terms responsible for the loops.

Within this simplified dynamics, a loop is initiated at a time  $s_0$  for which  $X_0 = X(s_0) < -1$  and  $Y_0 = Y(s_0) \ll |X_0|$ . The maximum distance from the stable line is attained at a time  $s^*$  for which  $X(s^*)$  is of the order of  $-Y(s^*)$ , that is when  $X(s^*) = -\beta Y(s^*)$ ,  $\beta$  being an arbitrary constant. When the noise is neglected, one straightforwardly obtains:  $Y(s)/X(s) = Y_0 Z_0 / \{X_0 Z_0 + (1 - e^{s_0-s}) [X_0^2 + Y_0^2]\}$  and the radius of the loop can be estimated as

$$|X(s^*)| = \frac{\beta [X_0 + Z_0] X_0^h}{[1 + \beta^2]^{(1+h)/2}} Y_0^{-h}. \quad (9)$$

For the trajectory to reach values  $X < x \ll -1$ , the radius has to be larger than  $-x$ , and thus  $Y(s_0)$  has to be smaller than  $|x|^{-1/h}$ . The joint PDF of  $X$  and  $Y$  at time

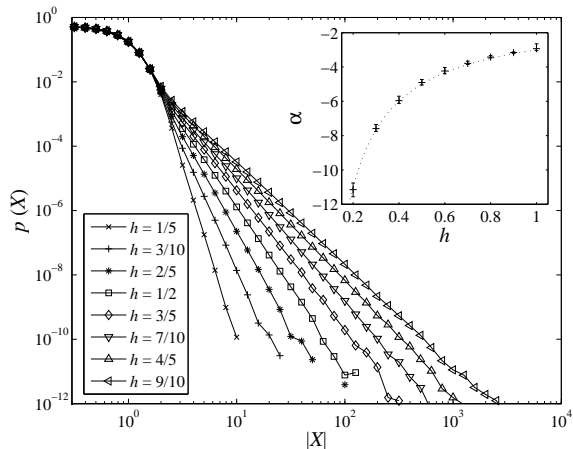


FIG. 3: PDF of  $X$  in log-log coordinates for  $\mathcal{S}(L) = 1$  and various values of  $h$ . In all cases, power-law tails are observed. Inset: exponent  $\alpha$  of the algebraic tail as a function of the fluid velocity Hölder exponent  $h$ ; the theoretical prediction is represented as a dotted line.

$s_0$  is given by the dynamics close to the line  $X = Y = 0$ . As it is finite for  $Y \rightarrow 0$ , the contribution (i) can be estimated to be  $\propto |x|^{-1/h}$ . The contribution (ii) can be obtained as follows. Far from the stable line, the dynamics can be approximated by the deterministic part, hence the fraction of time spent at  $X < x$  is  $\propto Y_0 \propto |x|^{-1/h}$ . Putting together the two contributions, we obtain that  $P^<(x) \propto |x|^{-2/h}$  when  $x \ll -1$ . The negative tail of the PDF of the longitudinal velocity difference  $X$  behaves as a power-law  $\propto |x|^{-\alpha}$  with  $\alpha = 1 + 2/h$ . This gives  $\alpha = 3$  for smooth flows ( $h = 1$ ) as previously derived [14]. During the large loops, the trajectories equally reach large positive values of  $X$  and of  $Y$ . This gives again a fraction of time  $x^{-1/h}$  spent at both  $X$  and  $Y$  larger than  $x \gg 1$ . Hence, the PDF of both the longitudinal and the transversal velocity differences have algebraic left and right tails.

As shown in Fig. 3, the presence of power-law tails in the PDF is confirmed numerically, with perfect agreement between the measured values of  $\alpha$  and the prediction  $\alpha = 1 + 2/h$  (see inset). Let us comment on the  $h$  dependence of this exponent  $\alpha$ . The large loops responsible for the algebraic tails correspond to events in which particles approach each other very closely; they are the basic mechanism of particle clustering. The probability to enter such loops decreases significantly when  $h \rightarrow 0$ . Moreover, it is straightforward to check from (6)-(8) that during the loops  $Z(s) \propto Z_0^h$  when  $Z_0 \ll 1$ . Hence it gets less and less probable to reach smaller values of  $Z$  as  $h$  decreases. Combined together, these two effects explain why particle clustering is weakened in rough velocity fields and why it is more efficient in smooth flows.

The change of variables (5) can be equally applied in three dimensions, leading to a dynamics different from (6)-(8). Therefore understanding to what extent the

above findings extend to the 3D case remains an open question; work in this direction is under development.

To conclude, let us comment on the implications of this work on the study of heavy particles in realistic turbulent flows. There, particle clustering is simultaneously due to ejection from eddies and to a dissipative dynamics. The considered model flow isolates the latter effect. It is probable that power-law tails for velocity differences can be present in realistic settings as well. However, it is not clear if the results on clustering are affected by the presence of persistent structures: particle ejection from eddies may form voids and thus very strong inhomogeneities in the particle distribution [10]. This could overtake dissipative-dynamics mechanisms.

We acknowledge useful discussions with L. Biferale, G. Falkovich, K. Gawędzki, A. Lanotte, S. Musacchio, and F. Toschi. This work has been partially supported by the EU network HPRN-CT-2002-00300 and by the French-Italian Galileo program “Transport and dispersion of impurities in turbulent flows”. The stay of R.H. in Nice was supported by the Zeiss-Stiftung and the DAAD.

- 
- [1] C. Crowe, M. Sommerfeld, and Y. Tsuji, *Multiphase Flows with Particles and Droplets* (CRC Press, New York, 1998).
  - [2] H. Pruppacher and J. Klett, *Microphysics of Clouds and Precipitation* (Kluwer Academic Publishers, Dordrecht, 1996).
  - [3] I. de Pater and J. Lissauer, *Planetary Science* (Cambridge University Press, Cambridge, 2001).
  - [4] U. Frisch, *Turbulence: The Legacy of A.N. Kolmogorov* (Cambridge University Press, Cambridge, 1995).
  - [5] J. Bec, *J. Fluid Mech.* **528**, 255 (2005).
  - [6] T. Elperin, N. Kleeorin, and I. Rogachevskii, *Phys. Rev. Lett.* **77**, 5373 (1996).
  - [7] E. Balkovsky, G. Falkovich, and A. Fouxon, *Phys. Rev. Lett.* **86**, 2790 (2001).
  - [8] J. Eaton and J. Fessler, *Int. J. Multiphase Flow* **20**, 169 (1994).
  - [9] G. Falkovich, A. Fouxon, and M. Stepanov, in *Sedimentation and Sediment Transport*, edited by A. Gyr and W. Kinzelbach (Kluwer Academic Publishers, Dordrecht, 2003), pp. 155–158.
  - [10] G. Boffetta, F. De Lillo, and A. Gamba, *Phys. Fluids* **16**, L20 (2004).
  - [11] H. Sigurgeirsson and A. Stuart, *Phys. Fluids* **14**, 4352 (2002).
  - [12] P. Fevrier, O. Simonin, and K. Squires, *J. Fluid Mech.* **533**, 1 (2005).
  - [13] M. Maxey, *J. Fluid Mech.* **174**, 441 (1987).
  - [14] J. Bec, M. Cencini, and R. Hillerbrand (2006), preprint.
  - [15] A. Fouxon and P. Horvai (2006), preprint.
  - [16] R. Kraichnan, *Phys. Fluids* **11**, 945 (1968).
  - [17] L. Piterbarg, *SIAM J. Appl. Math.* **62**, 777 (2002).
  - [18] B. Mehlig and M. Wilkinson, *Phys. Rev. Lett.* **92**, 250602 (2004).